HHS Public Access

Author manuscript

Bone. Author manuscript; available in PMC 2025 January 01.

Published in final edited form as:

Bone. 2025 January ; 190: 117326. doi:10.1016/j.bone.2024.117326.

Calorie restriction induces mandible bone loss by regulating mitochondrial function

Linyi Liu[a], **Phuong T. Le**[a], **Victoria E. DeMambro**[a], **Tiange Feng**[a], **Hanghang Liu**[b], **Wangyang Ying**[c], **Roland Baron**[d], **Clifford J. Rosen**[a,*]

[a]MaineHealth Institute for Research, Scarborough, ME 04074, USA

[b]West China Hospital of Stomatology, Sichuan University, Sichuan, China

[c]School of Computing and Augmented Intelligence, Arizona State University, Tempe, AZ 85281, USA

[d]Division of Bone and Mineral Research, Dept of Oral Medicine, Infection and Immunity, Harvard School of Dental Medicine, Boston, MA 02115, USA

Abstract

Caloric restriction (CR), commonly used as both a lifestyle choice and medical strategy, has been shown to adversely impact appendicular bone mass. However, its influence on alveolar bone health and the underlying mechanisms remain poorly understood. In this study, 8-week-old C57BL/6 J mice were fed with 30 % CR for 8 weeks. Micro-architecture, histologic parameters, and in vitro trajectories of osteoblast and adipocyte differentiation were examined. To further explore the underlying mechanisms, metabolic cages and in vitro bioenergetics were performed. Our results showed that 8 weeks of CR led to trabecular and cortical bone loss in the mandibles of female mice. CR in female mice decreased bone formation and bone resorption activities but induced adiposity in the mandibles. After CR, the adipogenesis in mesenchymal cells from orofacial bones (OMSCs) was greatly accelerated, whereas osteogenic differentiation was reduced in females. Undifferentiated CR OMSCs showed marked suppression in ATP production rates from mitochondria in female mice. ATP production rates decreased after osteogenesis but were upregulated during adipogenesis in female mice. Conversely, the generation of reactive oxygen species (ROS) was heightened during both osteoblastic and adipogenic differentiation in female CR groups. Collectively, our study indicated that CR could cause significant bone loss in the

*Corresponding author at: MaineHealth Institute for Research, 81 Research Drive, Scarborough, ME 04074, USA., Clifford.Rosen@mainehealth.org (C.J. Rosen).

Declaration of competing interest

The authors declared no potential conflicts of interest with respect to the research, authorship, and/or publication of this article.

CRediT authorship contribution statement

Linyi Liu: Writing – original draft, Visualization, Investigation, Formal analysis, Data curation, Conceptualization. **Phuong T. Le:** Writing – review & editing, Formal analysis, Data curation. **Victoria E. DeMambro:** Writing – review & editing, Investigation, Formal analysis, Data curation. **Tiange Feng:** Writing – review & editing, Formal analysis, Data curation. **Hanghang Liu:** Writing – review & editing, Formal analysis, Data curation. **Wangyang Ying:** Formal analysis, Data curation. **Roland Baron:** Writing – review & editing, Supervision, Project administration, Conceptualization. **Clifford J. Rosen:** Writing – review & editing, Supervision, Project administration, Funding acquisition, Conceptualization.

mandibles of female mice, almost certainly related to a reduced ATP supply and the unregulated generation of ROS.

Keywords

Calorie restriction; Alveolar bone loss; Bone-fat balance; Mesenchymal cells; Energy metabolism

1. Introduction

Caloric restriction (CR) is established as an effective intervention for weight reduction, mitigating hyperglycemia and insulin resistance, and augmenting longevity in mice [1,2]. This recognition has led to its growing popularity in both lifestyle choices and medical approaches. A report from the Centers for Disease Control and Prevention (CDC) revealed that between 2013 and 2016, 49.1 % of U.S. adults tried to lose weight. Moreover, among adults who tried to lose weight, the most commonly reported methods were exercising (62.9 %) and eating less food (62.9 %) [3]. However, an increasing body of studies indicates that CR should be used cautiously due to adverse effects on the skeleton, including a decrease in both bone quantity and bone quality [4,5]. In the CALERIE trial, modest CR showed 2 % lower bone mineral density (BMD) at the femoral neck, lumber spine, and total hip [6]. Likewise, in animal experiments, CR causes appendicular bone loss although the mechanism has not been defined [7,8]. Our previous study also showed that 30 % CR decreased cortical bone volume but didn't affect trabecular bone in the femora of female mice [9,10]. These findings suggested that the effects of CR could differ depending on anatomy, sex, age at CR initiation, and degree of dietary restriction.

The mandible, an unusual U-shaped bone that forms the base of the skull, is one example of an oral bone. It is the largest, strongest, and only movable bone of the skull. It serves as the anchor for the lower teeth and is essential for both mastication (chewing) and articulation (speaking). Compared with appendicular bones, the mandible has many unique features. First, as opposed to limb bones, which come from mesoderm, the mandible is derived from the cranial neural crest [11]. Second, the process of developmental ossification is different. The mandible develops through the process of both intramembranous and endochondral ossification, while bones in the appendicular skeleton form via endochondral ossification [12]. Third, in contrast to the appendicular bones, the mandible is subjected to more frequent and higher compressive forces in daily life [13].

In addition, it has also been demonstrated that the mandible has a higher amount of immature collagen, which gives it greater flexibility and increases its susceptibility to reconstruction [14]. In terms of cellular biological behavior, there is significant evidence showing that mesenchymal cells derived from orofacial bone/bone-marrow (OMSCs) exhibit a higher rate of proliferation, enhanced osteogenic capability, and lower potential for adipogenic differentiation compared to cells sourced from appendicular bones [15–17].

More importantly, the health of the mandible is closely related to various oral diseases, including periodontitis, periapical abscess, and osteonecrosis, as well as the key points of success for periodontal therapy, orthodontic treatments, and dental implants. However, it

is unknown if CR, would exert an adverse effect on the mandible, hence this study was designed to address that question.

2. Materials and methods

2.1. Ethics statement

All experimental procedures were approved by the Institutional Animal Care and Use Committee of the MaineHealth Institute for Research (IACUC #1914) and followed the US National Research Council's Guide for the Care and Use of Laboratory Animals, the US Public Health Service's Policy on Humane Care and Use of Laboratory Animals, and Guide for the Care and Use of Laboratory Animals.

2.2. Experimental animals

40 six-week-old male and female C57BL/6 J mice were obtained from The Jackson Laboratory (Bar Harbor, ME, USA) and kept in groups of five under specific pathogen-free conditions in a regulated environment at the MaineHealth Institute for Research's AAALAC-accredited facility. At eight weeks, mice were individually caged and randomly placed on either an ad libitum diet (AL, D10012Mi) or a 30 % calorie reduced (CR, D06112301i) diet (Research Diets, Inc., New Brunswick, NJ, USA) for 8 weeks, with CR mice receiving 70 % of the AL diet's daily food weight at 10 a.m. The diet for 30 % CR was formulated to ensure the provision of all essential vitamins and minerals while reducing carbohydrate intake. Weekly weight checks were conducted. The micro-CT and histological examination were performed by the third party without knowing the particular treatment each group received.

2.3. Dual-energy X-ray absorptiometry

Consistent with previous findings [10], mice underwent dual-energy X-ray absorptiometry (DXA) scans at 16 weeks of age using a PIXImus Densitometer (GE Lunar Corporation, Fairfield, CT, USA). A calibration with a manufacturer-provided phantom standard preceded each scan to ensure accuracy.

2.4. Microcomputed tomography

Following CR treatment for 8 weeks, mandibles and tibiae were extracted and conserved in 70 % ethanol for microcomputed tomography imaging. A high-resolution desktop micro-tomographic system (vivaCT 40, Scanco Medical AG, Brüttisellen, Switzerland) was used to assess the microarchitecture, mineral density, and volume of the trabecular and cortical bone in the mandibles and tibiae. The imaging was acquired using a standardized voxel size of 10.5 μm^3, with the x-ray tube's peak intensity set at 70 kVp, an electrical current of 114 mA, and a 250 ms integration time. Gaussian filtration and segmentation processes were applied to the scans. For the entirety of the research, Scanco's specialized software was employed. The region of interest in the trabecular bone of the mandibles was delineated by the areas surrounding the mesial and distal roots of the first mandibular molar, specifically below the furcation zone, across a buccal-lingual cross-section of the molar. The cortical bone region of interest was focused on the lingual side of the cortical bone. This area extends from the furcation region to the area above the embedded incisor, assessed on a

buccal-lingual cross-section of the first mandibular molar. In the trabecular bone of the tibiae, the region of interest for analysis commenced 105 μm (10 transverse slices) away from the growth plate break, stretching up to 1050 μm (100 transverse slices). For the cortical bone, the specified region of interest began 1995 μm proximal to the fibular junction and continued up to 525 μm (50 transverse slices) distally.

2.5. Histology

Following 8 weeks of CR, tissues including mandibles, tibiae, inguinal, gonadal white adipose tissue (iWAT, gWAT), and brown adipose tissue (BAT) were preserved in 10 % neutral buffered formalin overnight and subsequently placed in 70 % ethanol prior to histological processing. The technique for hematoxylin and eosin staining, previously detailed in our study (Maridas et al. 2019), was applied. Additionally, osteoclast staining was performed using the TRAP staining kit from Sigma (St. Louis, MO, USA), following the guidelines provided by the manufacturer.

2.6. Quantitative PCR

The total RNA was extracted from frozen iWAT, gWAT, mandibles, and femora using the Trizol technique (Thermo Fisher Scientific, Fairfield, CT). Following the manufacturer's protocol, complementary DNAs were synthesized from the RNA samples using the High-Capacity cDNA Reverse Transcription Kit (Thermo Fisher Scientific, Fairfield, CT) and then analyzed through quantitative polymerase chain reaction using a specialized supermix in a thermal cycler. Expression of the glyceraldehyde-3-phosphate dehydrogenase (Gapdh) served as the normalization reference for the targeted gene expressions, with the primer sequences provided in Appendix Table 1.

2.7. Enzyme-linked immunosorbent assay

Serum levels of procollagen type I amino-terminal propeptide (P1NP) and carboxy-terminal telopeptide of type I collagen (CTX) were measured using specific ELISA kits for mice (Immunodiagnostic Systems, Chicago, IL), as outlined in earlier research [18].

2.8. Cell culture, ALP, ORO, and ARS staining

After 8 weeks of CR, OMSCs were extracted from the mandibles, utilizing a method outlined in prior research [15]. Subsequently, the cells were incubated in Alpha Modified Eagle Medium (α-MEM) (GIBCO) enriched with 10 % FBS (GIBCO) and 1 % penicillin/streptomycin (GIBCO) at a temperature of 37 °C within a humidified atmosphere containing 5 % CO2. The cells at passage 1 were grown in either osteogenic (containing 50 μg/mL ascorbic acid and 8 mM beta-glycerophosphate) media for 7 and 14 days, or adipogenic (0.5 mM IBMX, 1 μM Dexamethasone, 10 μg/mL insulin, and 1 μM Rosiglitazone) media for 9 days, and then some cells were stained by alkaline phosphatase (ALP) staining, oil red O (ORO) staining, or alizarin red S staining (ARS). Other cells were isolated for detecting the osteogenic- and adipogenic-related genes by qRT-PCR or for mitochondrial tests.

Following the manufacturer's directions, the ALP staining was performed using a kit from Sigma-Aldrich (St. Louis, MO). For ARS staining, on the 14th day after initiating osteogenic differentiation, OMSCs were stained with a 1 % ARS solution at pH 4.2.

Subsequently, cells were cleared with a 10 % cetylpyridinium chloride solution, and the absorbance of the stained cells was measured at 562 nm.

For ORO staining, on the 9th day after adipogenic differentiation, adipocytes were fixed with 10 % neutral buffered formalin, then treated with 60 % isopropanol for 15 min at room temperature before staining with ORO solution. After staining, cells were washed several times for clear visualization. The isopropanol was used to extract lipids from the adipocyte droplets, and absorbance was measured at 490 nm.

2.9. Metabolic phenotyping

Metabolic assessments were conducted in the Pysiology Core at the MaineHealth Institute for Research utilizing the Promethion Metabolic Cage System (Sable Systems Intl., North Las Vegas, NV, USA), following methodologies outlined in our previous study [10]. Briefly, during the study, mice were kept under a 14-h light and 10-h dark cycle, starting with a 12-h acclimation phase, followed by a 72-h data collection phase. Data acquisition and instrument control were performed using the Promethion Live software version 23.0.5, and the obtained raw data were processed using Sable Systems Macro Interpreter version 22.10 using an analysis script detailing all aspects of data transformation. The results (energy expenditure (EE), respiratory exchange ratio (RER), water consumption, and activity) presented are the light, dark, and 24-h averages from this period. The 16-cage system used for the study includes cages with standard bedding, a food hopper, a water bottle, and an enrichment tube for measuring body mass, all connected to load cells for continuous monitoring. Additionally, an 11.5 cm running wheel was installed in each cage to track activity, with ambulatory movement and positioning monitored via XYZ beam arrays with closely spaced beams. AL-fed mice had ad libitum access to their diets, and mice in CR groups were fed at 10 a.m. every day.

2.10. Cellular fluorescence imaging

The mitochondrial content and reactive oxygen species (ROS) levels in undifferentiated, osteogenically differentiated (7 days), and adipogenically differentiated (9 days) OMSCs were evaluated using fluorescence imaging. This involved the application of 200 nM MitoTracker Red CMXRos (Invitrogen, Carlsbad, CA, USA) and 5 μM of CellROX (Invitrogen, Carlsbad, CA, USA), respectively. These dyes were incubated with the cells for 30 min at 37 °C, followed by capture using a Leica SP8 confocal microscope (Leica, Wetzlar, Germany). The quantitative analysis was performed in Image J.

2.11. Real-time metabolic analysis

OMSCs were isolated as above and plated at a density of 5000 cells/well in XF96 V3 PS cell culture microplates (Agilent Technologies, Santa Clara, CA, USA, #101085-004) and allowed to grow to confluency in growth media. Cells on half the plate were then assayed for mitochondrial function utilizing a mitochondrial stress test paradigm on the Seahorse XF96 Analyzer (Agilent). Oxygen consumption rate in cells was measured in basal conditions and in response to 1.25 μM of oligomycin (OLIGO), 1 μM of carbonyl cyanide-4 (trifluoromethoxy) phenylhydrazone (FCCP), and 0.5 μM of rotenone and antimycin A (ROT/AA). Data were analyzed using Wave Software V2.6 and Seahorse

XF Cell Mito Stress Test Report Generators (https://www.agilent.com). On the second half of the plate, cells were assayed for glycolytic function/ATP production rates, utilizing a combined glytolytic rate/ATP production rate assay paradigm. Basal OCR and extracellular acidification rates (ECAR) were measured and then in response to OLIGO (1.25 μM), ROT/AA (0.5 μM), and 2-deoxy-glucose (2-DG, 50 mM). Data were then analyzed using Seahorse XF Cell Glycolytic Rate/ATP Rate Report Generators. For the metabolic analysis of the osteogenic-differentiated and adipogenic-differentiated cells, OMSCs were first grown to confluency and then subjected to either osteoblast or adipocyte differentiation media for 7 or 9 days, respectively, prior to being assayed as above.

2.12. Statistical analysis

For statistical analysis, GraphPad Prism 9.0 (GraphPad Software) and SPSS 27 were utilized. An unpaired, two-tailed Student's *t*-test was employed for single comparisons. To determine the statistical significance of differences between more than two groups, one-way analysis of variance (ANOVA) was employed in conjunction with Sidak correction. A *P* value of less than 0.05 was deemed statistically significant.

3. Results

3.1. Calorie restriction significantly reduced body weight and bone mineral density

After 8 weeks of CR, it was observed that *the* body weights of mice subjected to CR were notably lower than those of mice in ad libitum (AL) groups in both males and females (Fig. 1a–c). Dual-energy X-ray absorptiometry (DXA) findings at 16 weeks of age indicated a significant decrease in whole body areal bone mineral content (aBMC), areal BMD, and femoral BMD in the CR groups compared to those in the AL groups (Fig. 1d–g). In terms of the changes in body composition, both lean weight and fat weight showed a marked reduction in CR groups in both sexes (Fig. 1d, f).

3.2. Calorie restriction resulted in bone loss in the mandibles of female mice

Micro-CT data showed that the mandible trabecular BMD (Tb. BMD), trabecular bone volume fraction (BV/TV), and cortical thickness (Ct.Th) of female mice were considerably reduced after 8 weeks of CR. But in male mice, CR did not cause bone loss (Fig. 2a, b, g, h). To compare whether CR had a differential impact on mandibles and long bones, we examined appendicular vs. oral bones by micro-CT, as illustrated in Fig. 2c–f, i, j, CR statistically decreased the Ct. Th in the tibiae but increased the Tb. BMD and BV/TV in females, opposing what was found in mandible trabecula. Furthermore, trabecular thickness (Tb.Th) and trabecular separation (Tb.Sp) in the tibiae were significantly reduced in the CR treatment groups, while these parameters remained unchanged in the mandibles. In male mice, CR reduced the Tb. BMD and thickness (Tb.Th) in the tibiae, while no effects of CR were noted in the mandible.

3.3. Calorie restriction inhibited bone formation and bone resorption of the mandibles in female mice

qRT-PCR analyses indicated that mandibles exhibited lower expression of osteogenesis-related genes such as *Col1a1*, *Runx2*, *Bglap,* and *Sp7* following 8 weeks of CR in female

mice (Fig. 3a). To further explore how CR affected the balance between osteoblastogenesis and osteoclastogenesis in mandibles, ELISA and histology assays were performed. The results from ELISA at 8 weeks post-CR revealed significant suppression of the bone formation marker P1NP and the bone resorption marker CTX in both male and female mice (Fig. 3b). H&E and TRAP staining suggested a notable reduction in the counts of osteoblast numbers (N.Ob/B. Pm), osteoblast surface (Ob.S/B.Pm), osteoclast numbers (N.Oc/B.Pm), and osteoclast surface (Oc.S/B·Pm) of mandibles in female mice after an 8-week period of CR (Fig. 3c, e, g, i). On the other hand, 8 weeks of CR significantly inhibited the processes of bone formation and resorption in the tibiae of both male and female mice (Fig. 3d, f, h, j).

3.4. Calorie restriction induced mandible bone marrow adiposity in females

To evaluate whether CR affected the adipose tissue in mandibles and long bones, tibiae and mandibles from both male and female mice were collected and subjected to histology after 8 weeks of CR. As shown in Fig. 4a, b, f, g, CR resulted in increased bone marrow adiposity in the tibiae of both male and female mice, while only female mandibles exhibited increased adipose area per marrow area (Ad.Ar/Ma.Ar). As expected, there was a significant decrease in the size of adipocytes in peripheral fat depots, including inguinal (iWAT), gonadal (gWAT), and brown adipose tissue (BAT) (Fig. 4c–e, h–j). In addition, qRT-PCR suggested that female mice' mandibles had much higher expression levels of adipogenic genes, including *Adiponectin*, *Cfd*, *Fabp4,* and *Plin2,* after 8 weeks of CR. Similarly, in both male and female mice, the expression of *Adiponectin*, *Pparγ*, *Cfd*, *Fabp4*, and *Cd36* was significantly upregulated in long bones like femora. However, in females, the levels of *Cfd* and *Plin2* decreased in both inguinal white adipose tissue (iWAT) and gonadal white adipose tissue (gWAT). In males, the expression of *Pparγ*, *Fabp4*, *Plin2*, and *Cd36* was significantly reduced in peripheral adipose tissue. (Fig. 4k–v).

3.5. Calorie restriction enhanced the adipogenic differentiation of OMSCs in females

In our previous study [9], we found that CR could promote the proliferation of BMSCs from appendicular bones, but in the present experiment, the results of crystal violet staining (CVS) indicated that CR didn't impact the growth rate of mesenchymal cells derived from orofacial bone (OMSCs) in both male and female mice (Fig. 5a, b, i). To investigate how CR affected the commitment of OMSCs, the ALP, ORO, ARS staining, and ALP quantitative assays were carried out. The findings revealed that CR could lead OMSCs to differentiate into adipocytes at the expense of osteoblasts in female mice, whereas CR had no effect on the direction of OMSCs differentiation in male mice (Fig. 5c–h, j–l). Additionally, qRT-PCR experiments were conducted to determine how CR influenced the expression of genes associated with osteogenesis and adipogenesis. As shown in Fig. 5m–q, the expressions of genes linked to osteogenesis, such as *Colα1*, *Runx2*, *Sp7*, *Bglap*, and *Spp1,* were reduced in CR groups, while the expressions of genes related to adipogenesis, such as *Adiponection*, *Pparγ*, and *Cfd,* were enhanced in female mice. However, in male mice, the expressions of the aforementioned genes did not alter in comparison to the AL groups (Fig. 5n–r).

3.6. Calorie restriction drove metabolic changes in both males and females

Since CR is the most straightforward and controlled approach to reducing energy intake, we performed metabolic cage studies to assess its effects on energy metabolism. As expected,

mice consuming fewer calories exhibited decreased dark cycle and 24-h total energy expenditure (EE) compared to mice fed ad libitum (AL), while EE during the light cycle remained unchanged in both male and female mice (Fig. 6a–d). Regression plots of total average EE versus body mass further confirmed distinct metabolic rates between males and females (Fig. 6a–d).

As a measure of substrate utilization, the respiratory exchange ratio (RER) indicated that CR-fed mice shifted their substrate use for energy production compared to AL-fed mice, (Fig. 6e, g). In addition, water consumption was significantly increased in CR-fed mice during the light cycle compared to the AL group (Fig. 6f, h).

In terms of activity, CR mice exhibited a marked increase in pedestrian movement and wheel-running behavior during the light phase (Fig. 6i–p). Wheel speed and pedestrian speed further confirmed that CR-fed mice showed higher levels of physical activity compared to their AL counterparts during the light cycle (Fig. 6i–p).

3.7. Calorie restriction altered mitochondrial respiration in female OMSCs

To better understand how CR influenced cellular energy metabolism, we performed cellular fluorescence imaging to quantify the mitochondrial membrane potential as well as reactive oxygen species (ROS) production and utilized real-time metabolic analysis for cellular bioenergetics in OMSCs. As demonstrated in Fig. 7a–c, e, throughout osteoblastic and adipogenic development, mitochondrial membrane potential of both the AL and CR groups increased in male OMSCs. On the other hand, following osteogenesis induction, mitochondrial function was decreased in female CR OMSCs, whereas it increased post-adipogenic differentiation. Compared with the cells in the AL groups, the OMSCs in the female CR groups enhanced the mitochondrial membrane potential during adipogenesis and lowered its function during osteoblastogenesis (Fig. 7b, c, e). In male mice and female AL groups, ROS generation was decreased during the osteogenesis phase but greatly increased during adipogenic differentiation (Fig. 7a–d). However, ROS production in both osteogenic and adipogenic differentiation of female mice was markedly raised after CR treatment (Fig. 7a–d). In contrast to the AL OMSCs, CR resulted in significantly elevated ROS generation during both osteogenic and adipogenic progression in female mice (Fig. 7b–d). Real-time oxygen consumption rate (OCR) and glycolytic rate measurements revealed that prior to differentiation, CR reduced the maximal respiration and spare respiratory capacity of female OMSCs, coupled with increased basal glycolytic rates and reductions in induced glycolytic capacities. These changes resulted in decreased mitoATP and increased glycoATP production rates. However, the increases in glycoATP were not sufficient to meet energy demands, resulting in a decrease in total ATP production rates (Fig. 7f). After 7 days of osteogenesis differentiation, basal, ATP-linked, and maximal mitochondrial respiration were reduced along with induced and compensatory glycolysis in female CR OMSCs. As a result, mitoATP production rates were significantly lower in the CR OMSCs, driving a reduction in overall ATP production rates compared to the AL female OMSCs (Fig. 7g). Interestingly, after 9 days of adipogenic differentiation, CR female OMSCs exhibited increased basal, ATP-linked, and maximal mitochondrial respiration with decreased glycolytic rates (Fig. 7h). In contrast to the osteogenic differentiated OMSCs, there was a notable improvement

in mitoATP production rates, driving an increase in total ATP production rates despite a significant decrease in glycoATP production rates in CR female OMSCs (Fig. 7h). In male mice, CR had no effect on mitochondrial function (Appendix Fig. 1).

4. Discussion

This is the first study to demonstrate that 30 % CR induces bone loss in the mandibles, but only in female mice, and adds to previous clinical and rodent studies on the detrimental effects of diet restriction on bone [19–22]. The observed sex-specific differences in mandibular bone are closely aligned with bioenergetic findings from mesenchymal stem cells derived from orofacial bone (OMSCs) in female C57BL/6 J mice. These changes in oral bone structure may have clinical importance in conditions such as periodontitis, implantology, and orthodontics. In this study, we demonstrated that in tibiae, cortical bone was most significantly reduced by CR in female mice. On the other hand, in terms of trabecular bone in tibiae, male mice exhibited a reduction in Tb.Th and BMD after 8 weeks of CR. Similarly, females showed a decrease in Tb.Th and Tb.Sp, but other trabecular-related parameters, such as Tb.BMD and BV/TV, were significantly increased. We postulated that reduced bone resorption was partially responsible for these changes in female mice between 8 and 16 weeks of age. These somewhat surprising results could be due to inhibition of accelerated age-related bone loss often observed in female C57BL/6 J mice during that time period and in higher bone remodeling areas such as trabecular bone [23]. In contrast to tibiae, CR only decreased the trabecular BMD, BV/TV, and cortical thickness of mandibles in female mice—not in males. Based on some previous studies, the average maximal bite force in men is around 30 % greater than in women [24]; this may explain some of the observed sex disparities. Furthermore, CR can change sex hormones and metabolic functions differently in males and females, which could also contribute to sex variability [25–27].

Bone formation and resorption play a crucial role in sustaining bone mass throughout the lifespan. We observed that CR decreased both osteoblast and osteoclast activity in female mandibles. Similarly, 8 weeks of CR were able to inhibit bone formation and bone resorption in the limbs but of both female and male mice. These data highlighted the distinct mechanisms driving CR-related bone loss in the mandibles compared to long bones.

The process by which CR causes bone loss remains unclear. Bone marrow adipose tissue (BMAT) represents over 10 % of the body’s total fat. Recent investigations demonstrated that BMAT has endocrine and paracrine activities [28–31]. During CR, BMAT in limb bones greatly increased, whereas peripheral adipose tissue diminished [7,9,32–34]. In the present study, BMAT in mandibles increased in females only. Since CR caused loss of mandibular bone in females only, it is possible that BMAT played a significant role in the CR-induced mandible loss. To get additional insight into the mechanisms underlying the buildup of BMAT in mandibles, the in vitro trajectories of osteoblast and adipocyte differentiation potentials of OMSCs were examined. According to CVS staining, CR had no effect on either sex’s ability to proliferate. However, the pace of adipogenesis in OMSCs was greatly accelerated, whereas osteogenic differentiation was reduced after 8 weeks of CR

in female mice. The augmentation of BMAT during CR may correlate with a preferential differentiation of OMSCs towards adipogenesis.

CR had a direct impact on energy metabolism, which was recognized as a crucial element in its effectiveness [35,36]. However, the energy transition and mitochondrial function in OMSCs have not been extensively studied. The data from metabolic chambers showed that CR-fed mice had a distinct metabolic signature from AL-fed mice. Mice of both sexes subjected to CR exhibited a reduction in total EE compared to those fed AL. The multiple linear regression displayed that the relative contribution of body mass to EE was different between females and males. The respiratory exchange ratio (RER), a measure of substrate oxidation, was different in the CR groups. The mice in our experiment fed with the CR diet showed a typical RER pattern, rising sharply to around 1.0 following refeeding and then falling to roughly 0.7–0.8 throughout the dark cycle, suggesting a greater reliance on lipids oxidation throughout the dark cycle. Following refeeding, the activity-related parameters—pedestrian meters, pedestrian speed, wheel meters, and wheel speed—were considerably elevated in the CR-fed groups. This heightened activity in the CR group could be an adaptive behavior to caloric restriction, indicating a potential compensatory mechanism to maintain energy balance. This may also help to explain why the value of EE during the daytime did not alter in CR groups. However, according to Abreu-Vieira et al. [37], activity only makes up approximately 10 % of mouse EE; therefore, the overall amount of EE was still lower in the CR groups.

To specifically investigate the metabolic changes in OMSCs following CR intervention, cellular fluorescence imaging alongside real-time metabolic assessments were performed. The MitoTracker staining showed the potential of the mitochondrial membrane was increased after osteogenic and adipogenic differentiation across both sexes in the AL-fed cohorts and in male CR groups. According to the MitoSOX fluorescence, ROS production would decrease during osteoblastic differentiation but increase during adipogenic induction for the groups mentioned, aligning with previous work [38,39]. In female CR groups, mitochondrial function was suppressed following osteogenic induction but enhanced after adipogenic differentiation. Concurrently, CR led to a rise in ROS generation during both osteogenic and adipogenic processes in female mice. While several earlier studies found no change or reduction in ROS levels following CR treatments, these studies were mainly focused on different tissues, such as the brain, heart, kidney, and liver [40]. Research conducted by Liu et al. [41] indicated that GHRKO mice exhibited an increased resistance to oxidative stress in muscles, kidneys, and livers, but ROS levels in osteocytes were significantly upregulated in female mice, which suggested that bone might have a unique metabolic response that is different from other bodily tissues. Furthermore, since OMSCs are the source of both osteoblasts and adipocytes, the increase in ROS levels observed during both osteogenic and adipogenic differentiation after an 8-week period of CR in female mice may elucidate the preference of OMSCs for developing into adipocytes over osteoblasts, due to ROS's established role in facilitating adipogenesis and impeding osteogenesis [38].

Glycolysis and oxidative phosphorylation (OXPHOS) are two major metabolic pathways that provide energy for cells. To clarify the energy transformation during this process, bioenergetics using seahorse technology was conducted. The results suggested that the

characteristics related to OCR during the mitochondrial stress test, such as maximal respiration and spare respiratory capacity, were significantly decreased in female CR groups before differentiation. Notably, the total ATP and mitochondrial ATP production rates were also decreased in CR groups, but ATP from glycolysis increased. This demonstrated the lack of ATP compelled OMSCs to raise glycolysis rates to partially offset the absence of mitochondrial energy production under the condition of CR. After 7 days of osteoblastic development, compared with the AL groups, the CR groups' respiratory parameters in both glycolysis and mitochondrial OXPHOS were dramatically suppressed in female mice. Likewise, total ATP and mitochondrial ATP were decreased. Interestingly, following 9 days of adipogenic differentiation, the CR female groups' mitochondrial respiratory parameters—such as basal, ATP-linked, and maximal respiration—significantly rose while the glycolysis-related measures declined. When it came to ATP synthesis, CR female OMSCs had higher total and mitochondrial ATP production rates, despite glycoATP production rates were decreased. This suggested that the OMSCs in the CR groups would primarily depend on OXPHOS for energy supply during adipogenesis. As previously reported, the maximal production from OXPHOS is 33.45 ATP/glucose, while glycolysis only generates 2 ATP/glucose after full oxidation of glucose [42]. This implies that in the CR environment, female OMSCs used a lot more energy to develop into adipocytes, resulting in a delay in osteoblast differentiation with CR.

5. Limitations

Our study primarily analyzed the cortical bone in the furcation area, with a specific focus on the lingual side, extending from the furcation region to the area above the embedded incisor. However, cortical bone in other regions, such as the buccal side, basal bone, and the alveolar bone surrounding the incisor, may respond differently to caloric restriction (CR), as these regions are predominantly cortical. Further research is needed to determine whether CR has similar effects across different regions of the mandible.

6. Conclusions

Our studies are the first to systematically evaluate the effects of CR on the mandibles. We conclude that CR drives trabecular and cortical bone loss in female mice only; this was related to the pattern of energy metabolism during this process. Further studies will be needed to clarify the sex differences in response to CR in oral bones and the impact on other oral diseases. This study emphasizes the importance for dental professionals to take their patients' CR history into account prior to treatment.

Supplementary Material

Refer to Web version on PubMed Central for supplementary material.

Acknowledgements

The authors disclosed receipt of the following financial support for the research, authorship, and/or publication of this article: This study was supported by NIAMS grant RO1AR073774 to Clifford J Rosen. This work utilized the services of the Physiology Core facilities at MHIR, supported by NIH/NIGMS P20GM121301.

Data availability

All data are available in the main text or the Supplementary Materials.

Appendix A

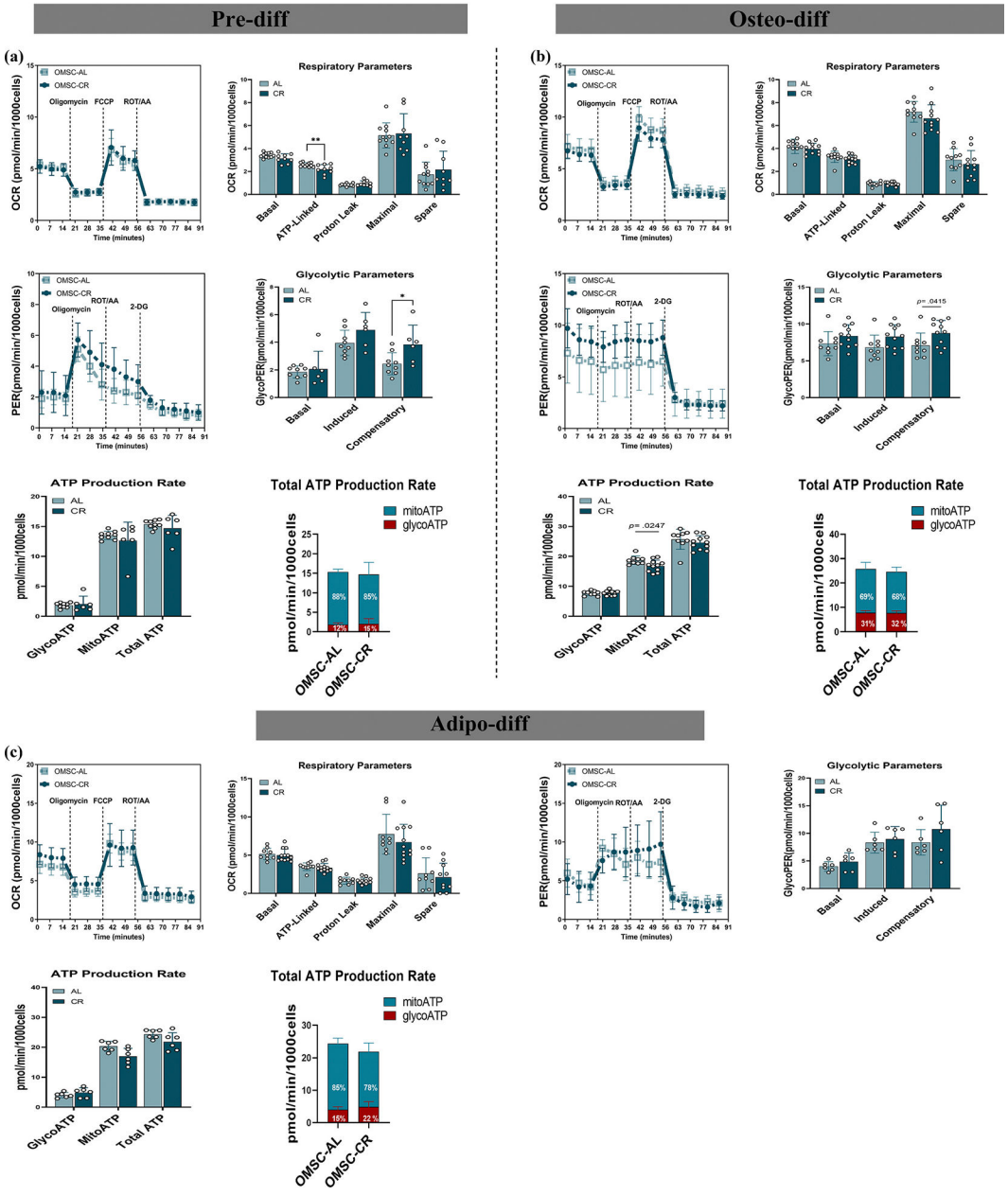

Appendix Fig. 1.

CR didn't affect the mitochondrial function in the OMSCs of male mice. (a-c) Seahorse technology indicated that neither the oxidative phosphorylation nor the glycolysis pathways were altered in undifferentiated or differentiated OMSCs of male mice. n = 6–11 cells/cohort.

Appendix Table 1

Primer sequences used in real-time polymerase chain reaction.

Primer	Sequence 5′-3′
Col1α1	F:5′- TCGTGGCTTCTCTGGTCTC-3′ R:5′- CCGTTGAGTCCGTCTTTGC-3′
Runx2	F:5′- ACCATAACAGTCTTCACAAATCCT-3′ R:5′- GAGGCGATCAGAGAACAAACTA-3′
Alpl	F:5′- GGTATGGGCGTCTCCACAGT-3′ R:5′- GCCCGTGTTGTGGTGTAGCT-3′
Bglap	F:5′- CTGACCTCACAGATGCCAAGC-3′ R:5′- TGGTCTGATAGCTCGTCACAAG-3′
Spp1	F:5′- CACTCCAATCGTCCCTACAGT-3′ R:5′- CTGGAAACTCCTAGACTTTGACC-3′
Sp7	F:5′- ATGGCGTCCTCTCTGCTTG-3′ R:5′- TTCCCCAGGGTTGTTGAGTC-3′
Adiponectin	F:5′- GATGGCACTCCTGGAGAG-3′ R:5′- GCTCCTGTCATTCCAACATC-3′
Ppar-γ	F:5′- CTGCCTATGAGCACTTCACAAG-3′ R:5′- CTCTTGTGAATGGAATGTCTTCA-3′
Cfd	F:5′- CATGCTCGGCCCTACATGG-3′ R:5′- CACAGAGTCGTCATCCGTCAC-3′
Fabp4	F:5′- CAGGTGCAGAAGTGGGATG-3′ R:5′- AGTCACGCCTTTCATAACAC-3′
Plin2	F:5′- TCAGGATAAGCTCTATGTCTCGTG-3′ R:5′- CCTGATCTTGAATGTTCTGTGGT-3′
Cd36	F:5′- GGAGCCATCTTTGAGCCTTCA-3′ R:5′- GAACCAAACTGAGGAATGGATCT-3′
Gapdh	F:5′- AACGACCCCTTCATTGACCT-3′ R:5′- ATGTTAGTGGGGTCTCGCTC-3′

Alpl, alkaline phosphatase; *Bglap*, bone gamma carboxyglutamate protein; *Cfd*, complement factor D; *Col1α1*, collagen, type I, alpha 1; *Fabp4*, fatty acid binding protein 4; F, forward; *Gapdh*, glyceraldehyde-3-phosphate dehydrogenase; *Plin2*, perilipin 2; *Ppar-γ*, peroxisome proliferator activated receptor gamma; R, reverse; *Runx2*, runt related transcription factor 2; *Sp7*, Sp7 transcription factor 7; *Spp1*, secreted phosphoprotein 1.

References

[1]. Mattison JA, Colman RJ, Beasley TM, Allison DB, Kemnitz JW, Roth GS, Ingram DK, Weindruch R, de Cabo R, Anderson RM, Caloric restriction improves health and survival of rhesus monkeys, Nat. Commun. 8 (2017) 14063. [PubMed: 28094793]

[2]. Redman LM, Smith SR, Burton JH, Martin CK, Il'yasova D, Ravussin E, Metabolic slowing and reduced oxidative damage with sustained caloric restriction support the rate of living and oxidative damage theories of aging, Cell Metab. 27 (2018) 805–815.e4. [PubMed: 29576535]

[3]. Martin CB, Herrick KA, Sarafrazi N, Ogden CL, Attempts to lose weight among adults in the United States, 2013–2016, NCHS Data Brief 313 (2018) 1–8.

[4]. Schwartz AV, Johnson KC, Kahn SE, Shepherd JA, Nevitt MC, Peters AL, Walkup MP, Hodges A, Williams CC, Bray GA, et al. , Effect of 1 year of an intentional weight loss intervention on bone mineral density in type 2 diabetes: results from the look AHEAD randomized trial, J. Bone Miner. Res. 27 (2012) 619–627. [PubMed: 22354851]

[5]. Faje AT, Karim L, Taylor A, Lee H, Miller KK, Mendes N, Meenaghan E, Goldstein MA, Bouxsein ML, Misra M, et al. , Adolescent girls with anorexia nervosa have impaired cortical and trabecular microarchitecture and lower estimated bone strength at the distal radius, J. Clin. Endocrinol. Metab. 98 (5) (2013) 1923–1929. [PubMed: 23509107]

[6]. Villareal DT, Fontana L, Das SK, Redman L, Smith SR, Saltzman E, Bales C, Rochon J, Pieper C, Huang M, et al. , Effect of two-year caloric restriction on bone metabolism and bone mineral density in non-obese younger adults: a randomized clinical trial, J. Bone Miner. Res. 31 (2016) 40–51. [PubMed: 26332798]

[7]. Devlin MJ, Cloutier AM, Thomas NA, Panus DA, Lotinun S, Pinz I, Baron R, Rosen CJ, Bouxsein ML, Caloric restriction leads to high marrow adiposity and low bone mass in growing mice, J. Bone Miner. Res. 25 (2010) 2078–2088. [PubMed: 20229598]

[8]. Behrendt AK, Kuhla A, Osterberg A, Polley C, Herlyn P, Fischer DC, Scotland M, Wree A, Histing T, Menger MD, et al. , Dietary restriction-induced alterations in bone phenotype: effects of lifelong versus short-term caloric restriction on femoral and vertebral bone in C57BL/6 mice, J. Bone Miner. Res. 31 (2016) 852–863. [PubMed: 26572927]

[9]. Liu L, Le PT, Stohn JP, Liu H, Ying W, Baron R, Rosen CJ, Calorie restriction in mice impairs cortical but not trabecular peak bone mass by suppressing bone remodeling, J. Bone Miner. Res. 12 (2024) zjae104.

[10]. Maridas DE, Rendina-Ruedy E, Helderman RC, DeMambro VE, Brooks D, Guntur AR, Lanske B, Bouxsein ML, Rosen CJ, Progenitor recruitment and adipogenic lipolysis contribute to the anabolic actions of parathyroid hormone on the skeleton, FASEB J. 33 (2019) 2885–2898. [PubMed: 30354669]

[11]. Yuan Y, Chai Y, Regulatory mechanisms of jaw bone and tooth development, Curr. Top. Dev. Biol. 133 (2019) 91–118. [PubMed: 30902260]

[12]. Karaplis A, Embryonic development of bone and the molecular regulation of intramembranous and endochondral bone formation, Principles of Bone Biology. (2002) 33–58.

[13]. de Jong WC, Korfage JA, Langenbach GE, Variations in habitual bone strains in vivo: Long bone versus mandible, J. Struct. Biol. 172 (2010) 311–318. [PubMed: 20600955]

[14]. Matsuura T, Tokutomi K, Sasaki M, Katafuchi M, Mizumachi E, Sato H, Distinct characteristics of mandibular bone collagen relative to long bone collagen: relevance to clinical dentistry, Biomed. Res. Int. 2014 (2014) 769414. [PubMed: 24818151]

[15]. Yamaza T, Ren G, Akiyama K, Chen C, Shi Y, Shi S, Mouse mandible contains distinctive mesenchymal stem cells, J. Dent. Res. 90 (2011) 317–324. [PubMed: 21076121]

[16]. Eber MR, Park SH, Contino KF, Patel CM, Hsu FC, Shiozawa Y, Osteoblasts derived from mouse mandible enhance tumor growth of prostate cancer more than osteoblasts derived from long bone, J Bone Oncol. 26 (2021) 100346. [PubMed: 33425674]

[17]. Lin W, Li Q, Zhang D, Zhang X, Qi X, Wang Q, Chen Y, Liu C, Li H, Zhang S, et al. , Mapping the immune microenvironment for mandibular alveolar bone homeostasis at single-cell resolution, Bone Res. 15;9(1):17 (2021). [PubMed: 33723232]

[18]. Liu L, Leng S, Yue J, Lu Q, Xu W, Yi X, Huang D, Zhang L, EDTA enhances stromal cell-derived factor 1α-induced migration of dental pulp cells by up-regulating chemokine receptor 4 expression, J. Endod. 45 (5) (2019) 599–605.e1. [PubMed: 30926162]

[19]. Devlin MJ, Brooks DJ, Conlon C, Vliet Mv L. Louis, C.J. Rosen ML Bouxsein, Daily leptin blunts marrow fat but does not impact bone mass in calorie-restricted mice, J. Endocrinol. 229 (2016) 295–306. [PubMed: 27340200]

[20]. Aaron N, Kraakman MJ, Zhou Q, Liu Q, Costa S, Yang J, Liu L, Yu L, Wang L, He Y, et al. , Adipsin promotes bone marrow adiposity by priming mesenchymal stem cells, Elife 10 (2021) e69209. [PubMed: 34155972]

[21]. Liu L, Rosen CJ, New insights into calorie restriction induced bone loss, Endocrinol Metab (Seoul). 38 (2) (2023) 203–213. [PubMed: 37150516]

[22]. Bredella MA, Fazeli PK, Bourassa J, Rosen CJ, Bouxsein ML, Klibanski A, Miller KK, The effect of short-term high-caloric feeding and fasting on bone microarchitecture, Bone 154 (2022) 116214. [PubMed: 34571202]

[23]. Glatt V, Canalis E, Stadmeyer L, Bouxsein ML, Age-related changes in trabecular architecture differ in female and male C57BL/6J mice, J. Bone Miner. Res. 22 (8) (2007) 1197–1207. [PubMed: 17488199]

[24]. Palinkas M, Nassar MS, Cecílio FA, Siéssere S, Semprini M, Machado-de-Sousa JP, Hallak JE, Regalo SC, Age and gender influence on maximal bite force and masticatory muscles thickness, Arch. Oral Biol. 55 (10) (2010) 797–802. [PubMed: 20667521]

[25]. Słuczanowska-Głąbowska S, Laszczyńska M, Piotrowska K, Grabowska M, Grymuła K, Ratajczak MZ. 2015. Caloric restriction increases ratio of estrogen to androgen receptors expression in murine ovaries–potential therapeutic implications. J. Ovarian Res. 13; 8:57.

[26]. Sun J, Shen X, Liu H, Lu S, Peng J, Kuang H, Caloric restriction in female reproduction: is it beneficial or detrimental? Reprod. Biol. Endocrinol. 4;19(1):1 (2021). [PubMed: 33397418]

[27]. Suchacki KJ, Thomas BJ, Ikushima YM, Chen KC, Fyfe C, Tavares AAS, Sulston RJ, Lovdel A, Woodward HJ, Han X, The effects of caloric restriction on adipose tissue and metabolic health are sex- and age-dependent, Elife 25 (12) (2023) e88080.

[28]. Cawthorn WP, Scheller EL, Learman BS, Parlee SD, Simon BR, Mori H, Ning X, Bree AJ, Schell B, Broome DT, et al. , Bone marrow adipose tissue is an endocrine organ that contributes to increased circulating adiponectin during caloric restriction, Cell Metab. 20 (2014) 368–375. [PubMed: 24998914]

[29]. Deng P, Yuan Q, Cheng Y, Li J, Liu Z, Liu Y, Li Y, Su T, Wang J, Salvo ME, et al. , Loss of KDM4B exacerbates bone-fat imbalance and mesenchymal stromal cell exhaustion in skeletal aging, Cell Stem Cell 28 (2021) 1057–1073.e7. [PubMed: 33571444]

[30]. Fan Y, Hanai JI, Le PT, Bi R, Maridas D, DeMambro V, Figueroa CA, Kir S, Zhou X, Mannstadt M, et al. , Parathyroid hormone directs bone marrow mesenchymal cell fate, Cell Metab. 25 (2017) 661–672. [PubMed: 28162969]

[31]. Liu H, Liu L, Rosen CJ, PTH and the regulation of mesenchymal cells within the bone marrow niche, Cells 13 (5) (2024) 406. [PubMed: 38474370]

[32]. Larson-Meyer DE, Heilbronn LK, Redman LM, Newcomer BR, Frisard MI, Anton S, Smith SR, Alfonso A, Ravussin E, Effect of calorie restriction with or without exercise on insulin sensitivity, beta-cell function, fat cell size, and ectopic lipid in overweight subjects, Diabetes Care 29 (2006) 1337–1344. [PubMed: 16732018]

[33]. Fazeli PK, Bredella MA, Pachon-Peña G, Zhao W, Zhang X, Faje AT, Resulaj M, Polineni SP, Holmes TM, Lee H, et al. , The dynamics of human bone marrow adipose tissue in response to feeding and fasting, JCI Insight 6 (2021) e138636. [PubMed: 33974568]

[34]. Li Z, Bowers E, Zhu J, Yu H, Hardij J, Bagchi DP, Mori H, Lewis KT, Granger K, Schill RL, et al. , Lipolysis of bone marrow adipocytes is required to fuel bone and the marrow niche during energy deficits, Elife 11 (2022) e78496. [PubMed: 35731039]

[35]. Bruss MD, Khambatta CF, Ruby MA, Aggarwal I, Hellerstein MK, Calorie restriction increases fatty acid synthesis and whole body fat oxidation rates, Am. J. Physiol. Endocrinol. Metab. 298 (1) (2010) E108–E116. [PubMed: 19887594]

[36]. Pak HH, Haws SA, Green CL, Koller M, Lavarias MT, Richardson NE, Yang SE, Dumas SN, Sonsalla M, Bray L, Fasting drives the metabolic, molecular and geroprotective effects of a calorie-restricted diet in mice, Nat. Metab. 3 (10) (2021) 1327–1341. [PubMed: 34663973]

[37]. Abreu-Vieira G, Xiao C, Gavrilova O, Reitman ML, Integration of body temperature into the analysis of energy expenditure in the mouse, Mol. Metab. 4 (6) (2015) 461–470. [PubMed: 26042200]

[38]. Atashi F, Modarressi A, Pepper MS, The role of reactive oxygen species in mesenchymal stem cell adipogenic and osteogenic differentiation: a review, Stem Cells Dev. 24 (10) (2015) 1150–1163. [PubMed: 25603196]

[39]. Gao J, Feng Z, Wang X, Zeng M, Liu J, Han S, Xu J, Chen L, Cao K, Long J, et al. , SIRT3/SOD2 maintains osteoblast differentiation and bone formation by regulating mitochondrial stress, Cell Death Differ. 25 (2) (2018) 229–240. [PubMed: 28914882]

[40]. Walsh ME, Shi Y, Van Remmen H, The effects of dietary restriction on oxidative stress in rodents, Free Radic. Biol. Med. 66 (2014) 88–99. [PubMed: 23743291]

[41]. Liu Z, Solesio ME, Schaffler MB, Frikha-Benayed D, Rosen CJ, Werner H, Kopchick JJ, Pavlov EV, Abramov AY, Yakar S, Mitochondrial function is compromised in cortical bone osteocytes of Long-lived growth hormone receptor null mice, J. Bone Miner. Res. 34 (1) (2019) 106–122. [PubMed: 30216544]

[42]. Mookerjee SA, Gerencser AA, Nicholls DG, Brand MD, Quantifying intracellular rates of glycolytic and oxidative ATP production and consumption using extracellular flux measurements, J. Biol. Chem. 292 (17) (2017) 7189–7207. [PubMed: 28270511]

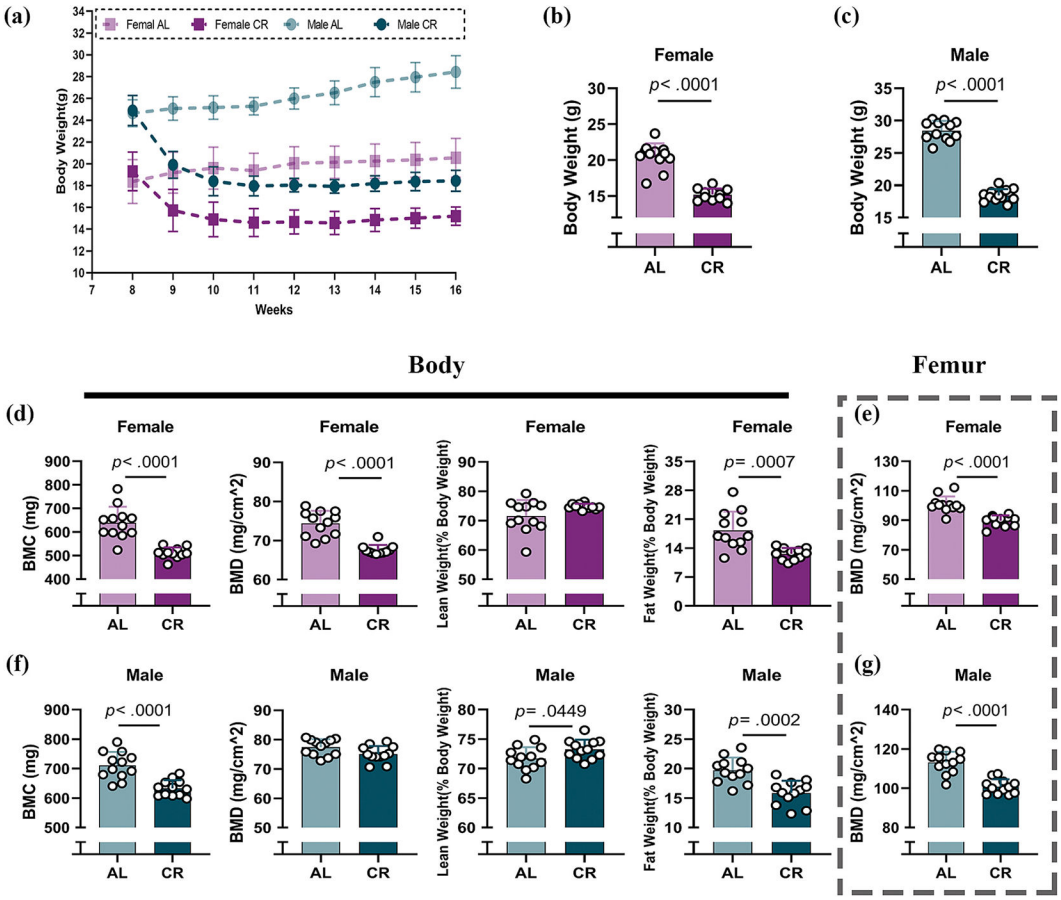

Fig. 1.

CR led to notable decreases in both body weight and femoral bone mineral density (BMD). (a–c) The body weights of mice under CR were notably lower than those of AL-fed mice after 8 weeks. (d–g) For both males and females, CR dramatically reduced femoral BMD. n = 10–12/cohort.

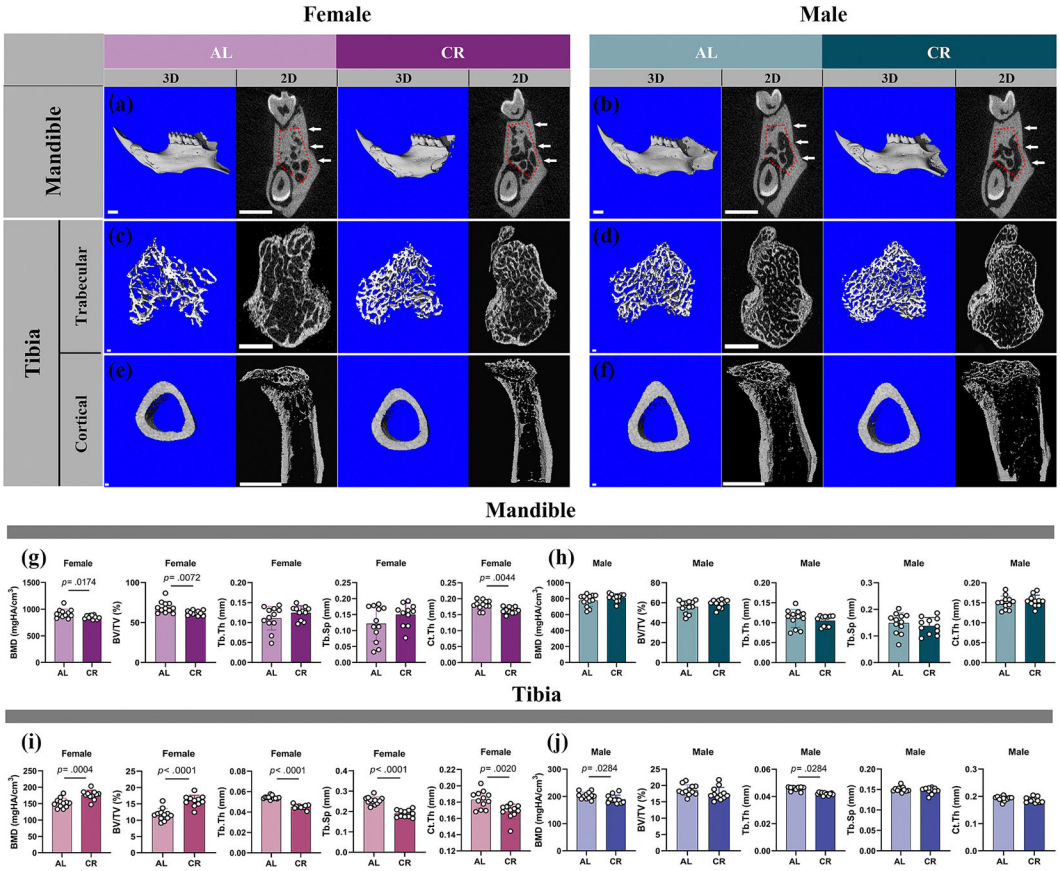

Fig. 2.

8 weeks of CR led to bone loss in the mandibles of female mice. (a, b) Two-dimensional (2D) and three-dimensional (3D) microarchitecture images of mandibles in both female and male mice. Scale bar, 1000 μm. ROI for trabecular bones was circled by red dashes. White arrows represented the region for cortical analysis. (c–f) Micro-CT was used to assess how CR affected the tibiae. Scale bar, 2D:1000 μm, 3D: 100 μm. (g) CR significantly decreased trabecular- and cortical-related parameters in the mandibles of female mice. (h) CR didn't affect the mandibles in male mice. (i) Trabecular BMD and BV/TV were increased in the tibiae of female mice after CR treatment. (j) CR reduced tibial Tb.BMD in male mice. n = 11–12/cohort. (For interpretation of the references to colour in this figure legend, the reader is referred to the web version of this article.)

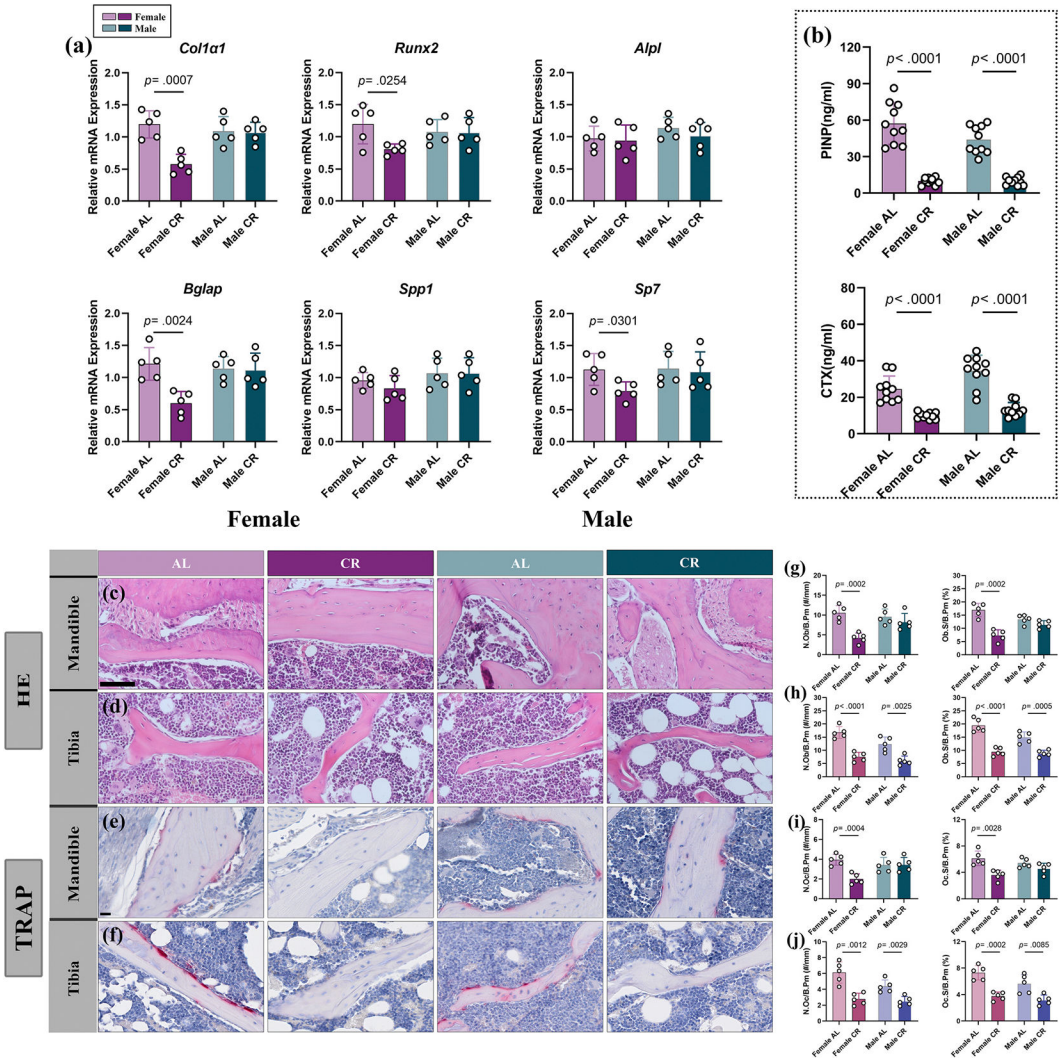

Fig. 3.

8 weeks of CR suppressed the bone formation and bone resorption of mandibles in females. (a) CR for 8 weeks significantly lowered the expression of osteogenesis-related genes in the mandibles of female mice. n = 5/cohort. (b) CR led to a reduction in serum levels of P1NP and CTX markers in both male and female mice. n = 10/cohort. (c–f) Representative HE (scale bar, 100 μm) and TRAP (scale bar, 20 μm) images of mandibles and tibiae in female and male mice. (g–j) Osteoblast and osteoclast activity of female mandibles was dramatically inhibited by CR. n = 5/cohort.

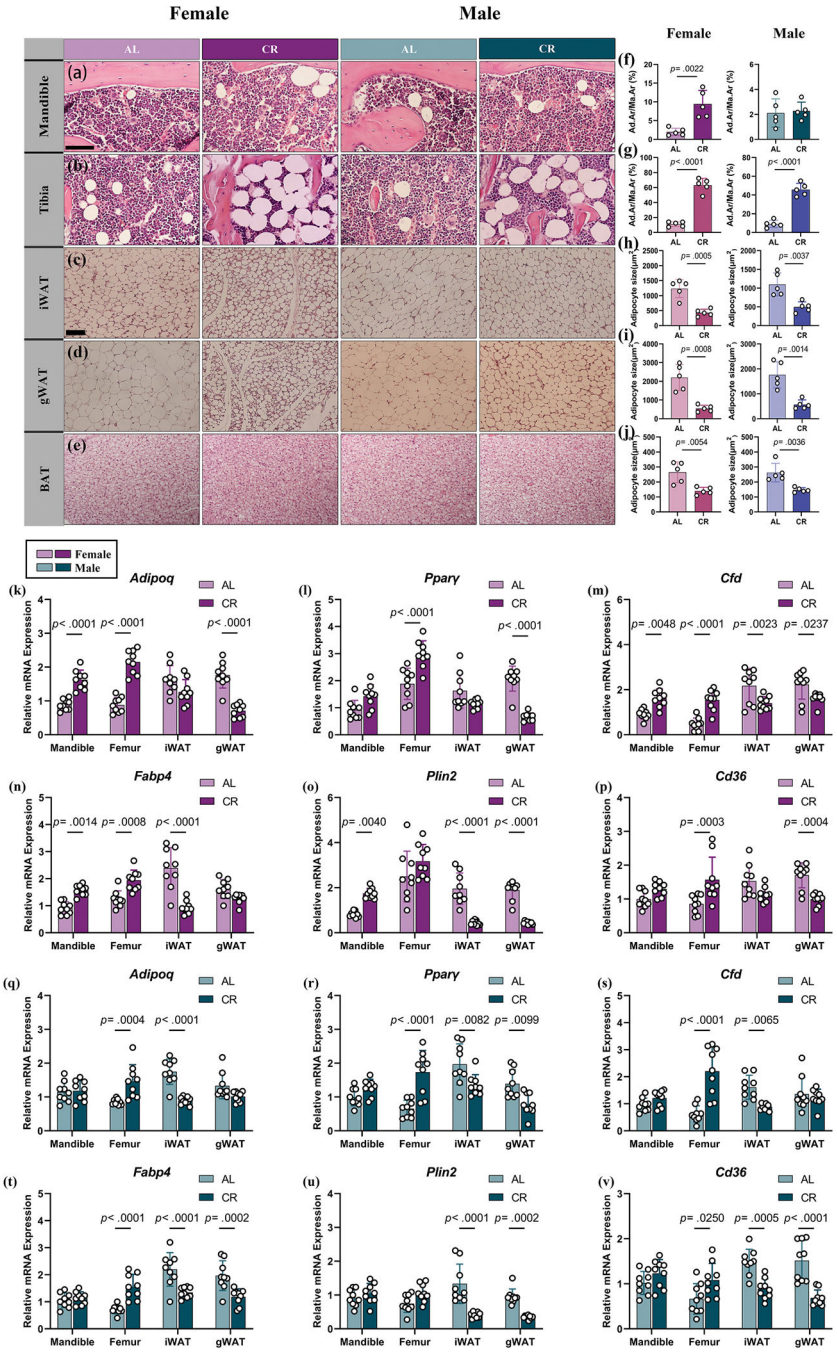

Fig. 4.

8 weeks of CR led to bone marrow adiposity in the mandibles of female mice. (a-e) Representative HE images of BMAT in both mandibles and the tibiae, iWAT, gWAT, and BAT in male and female mice. Scale bar, 100 μm. (f) The adipose area per marrow area (Ad.Ar/Ma.Ar) was increased in the CR group mandibles of female mice. n = 5/cohort. (g) CR induced BMAT accrual in the tibiae of both female and male mice. n = 5/cohort. (h-j) The adipocyte size of peripheral adipose was dramatically decreased following CR

treatment. n = 5/cohort. (k-v) The adipogenic-related genes in mandibles were significantly upregulated after 8 weeks of CR in female mice. n = 9/cohort.

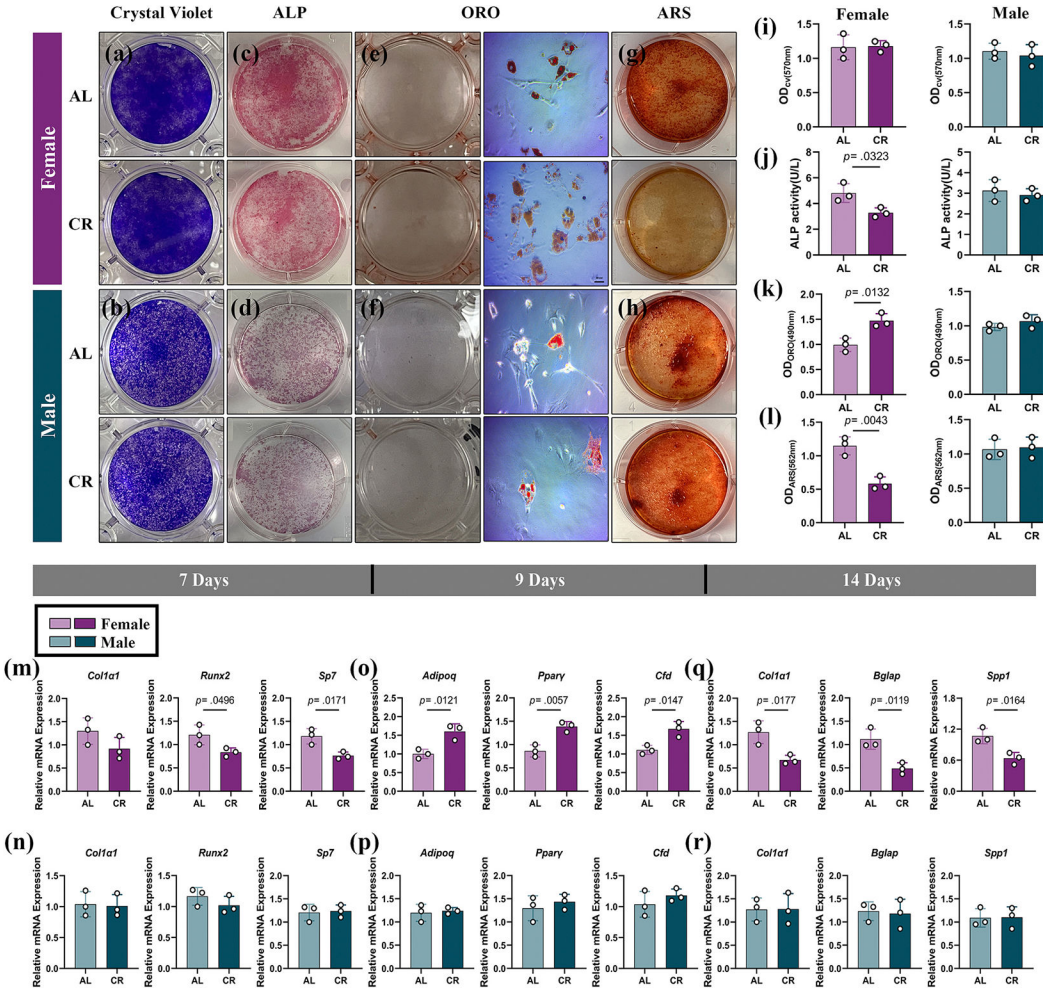

Fig. 5.

CR induced a lineage shift in female orofacial bone-derived mesenchymal cells (OMSCs), driving their differentiation from osteoblasts towards adipocytes. (a, b, i) CR didn't affect the proliferation potential of female and male OMSCs. n = 3/cohort. (c–l) ALP staining, ALP quantitative assay, ORO staining, and ARS staining suggested 8 weeks of CR promoted adipogenic differentiation at the expense of osteogenic differentiation in OMSCs of female mice. n = 3/cohort. (m–r) Following osteoblastic induction for 7 and 14 days and adipogenic differentiation for 9 days, the expressions of genes related to adipogenesis were upregulated while osteogenesis-related genes were downregulated. n = 3/cohort.

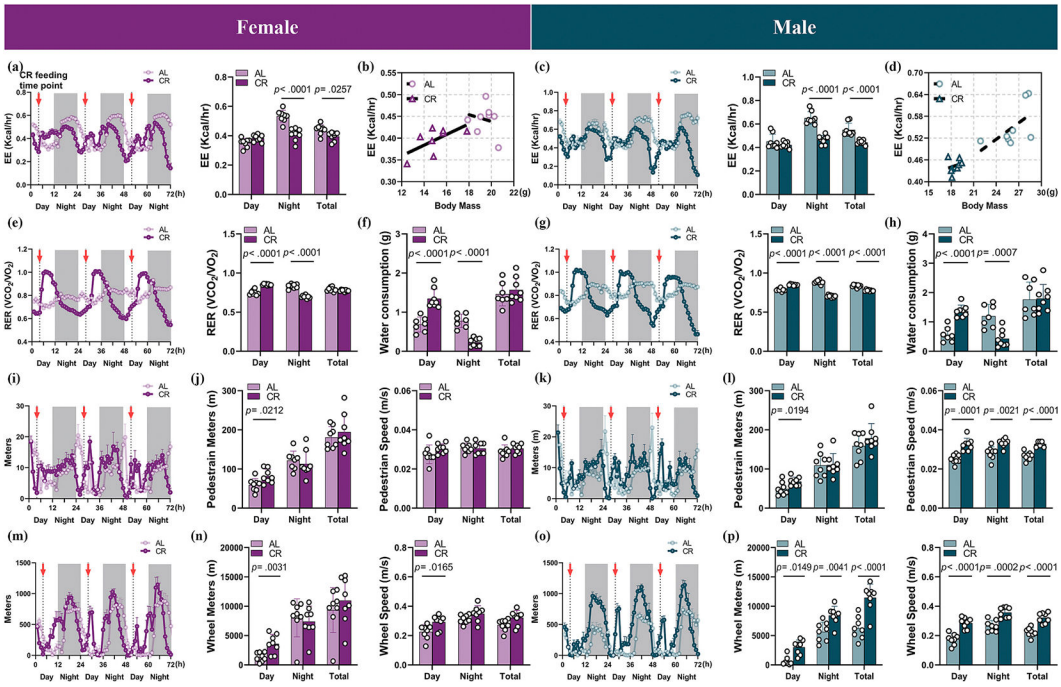

Fig. 6.

Energy metabolism was changed after 8 weeks of CR in both females and males. (a, c) Energy expenditure (EE) was decreased after CR treatment. n = 8/cohort. (b, d) Regression models showed females and males had different contributions of body mass to EE. n = 8/cohort. (e, g) The respiratory exchange ratio (RER) was changed in both males and females after 8 weeks of CR. n = 8/cohort. (f, h–p) The water consumption and activity were significantly increased right after the refeeding in both sex mice. n = 7–8/cohort.

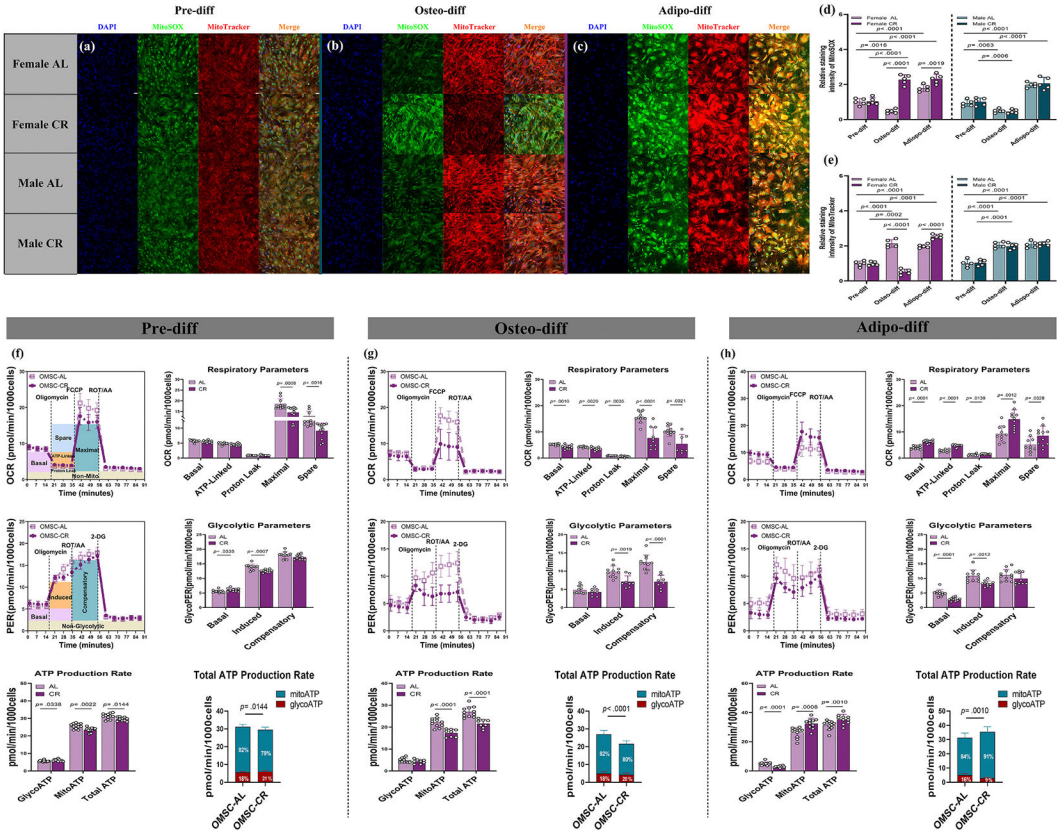

Fig. 7.

CR induced an imbalance of ROS production and ATP production rates in female OMSCs. (a–e) Inflorescence imaging of ROS and mitochondria indicated that 8 weeks of CR decreased the mitochondrial membrane potential during osteogenic differentiation while enhancing after-adipogenesis differentiation in female OMSCs. Meanwhile, ROS production was significantly elevated following both osteogenic and adipogenic induction in female OMSCs after CR. Scale bar, 5 μm, n = 5/cohort. (f) OCR, glycoPER, and ATP production rates were measured by seahorse technology prior to differentiation. n = 10–12 wells/cohort. (g) 8 weeks of CR inhibited both oxidative phosphorylation and glycolysis pathways in female OMSCS after osteogenic induction. n = 8–12 wells/cohort. (h) During adipogenesis, oxidative phosphorylation was the main source of energy for the OMSCs in the CR groups of female mice. n = 10–12 wells/cohort.